Wake control with permeable multilayer structures: The spherical symmetry case

Patrick T. Bowen,* David R. Smith, and Yaroslav A. Urzhumov
Center for Metamaterials and Integrated Plasmonics and Department of Electrical and Computer Engineering, Duke University, P.O. Box 90291, Durham, North Carolina 27708, USA
(Received 26 January 2015; revised manuscript received 14 May 2015; published 30 December 2015)

We explore the possibility of controlling the wake and drag of a spherical object independently of each other, using radial distributions of permeability in the Brinkman-Stokes formalism. By discretizing a graded-permeability shell into discrete, macroscopically homogeneous layers, we are able to sample the entire functional space of spherically-symmetric permeabilities and observe quick convergence to a certain manifold in the wake-drag coordinates. Monte Carlo samplings with 10^4–10^5 points have become possible thanks to our new algorithm, which is based on exact analytical solutions for the Stokes flow through an arbitrary multilayer porous sphere. The algorithm is not restricted to the Brinkman-Stokes equation and can be modified to account for other types of scattering problems for spherically-symmetric systems with arbitrary radial complexity. Our main practical finding for Stokes flow is that it is possible to reduce a certain measure of wake of a spherical object without any energy penalty and without active (power-consuming) force generation.

DOI: 10.1103/PhysRevE.92.063030 PACS number(s): 47.15.gm, 47.15.Tr

I. INTRODUCTION

Wake of an obstacle in a stationary flow is of interest because of both its fundamental importance in fluid dynamics and its direct impact on vessel design. In ship hydrodynamics, the magnitude of wake determines the key performance metrics of vessels, such as their drag coefficient and energy efficiency, as well as their maneuverability and even visibility. In small-scale hydrodynamics (e.g., microfluidics), wake and drag coefficients are important in the determination of effective viscosity and other properties of colloidal mixtures. While ship hydrodynamics generally deals with high-Re flows, which are both highly nonlinear and turbulent, microfluidic applications can benefit from the understanding of the Stokes (low-Re) limit [1]. The ability to control any wake-related metrics of small solid objects moving in fluids could impact the field of fluid rheology, leading to liquid media with novel properties, and shed light on the process of wake manipulation beyond the Stokes limit.

Stokes flow and its generalization, Brinkman-Stokes flow [2], have been studied extensively from the primary standpoint of hydrology, which deals with creeping flows through permeable soils and rocks [3,4]. Unsteady and oscillatory Brinkman-Stokes flows are also important in acoustics of porous structures [5,6]. A substantial effort was already devoted to the homogenization theory of saturated and unsaturated flows in porous media [7–9]. Through this effort, a rigorous definition of permeability—an effective parameter describing a fluid-saturated porous medium—has been produced. Permeability can be physically defined as the coefficient of proportionality between the force exerted by the solid component on the fluid and the macroscopic average flow velocity. At least in the linear (Stokes) limit, this proportionality has to be linear, making permeability a well-defined notion and a self-property of the porous medium in that regime [10]. Notably, this linear coefficient can be a second-rank tensor, as it relates two vector fields. Statistically anisotropic porous media are thus described by three principal permeabilities and an orthogonal vector basis in which the permeability tensor is diagonal.

Brinkman originally confirmed his generalization of Stokes flow by comparing with measurements of viscous forces on dense swarms of particles [11]. More recently, the Brinkman term has been experimentally confirmed by measurements of the settling velocity of porous spheres made of steel wool [12], which was analytically predicted in Ref. [8]. Within the context of layered structures, the drag force on solid spheres coated with a single layer of permeable material has also been measured and found to agree with the Brinkman-Stokes theory, where the permeable material was composed of polyester threads that were attached to the impermeable sphere [13].

In this paper, we analyze stationary Stokes flow past (and through) a spherically-symmetric solid with an arbitrary radial distribution of permeability. Several authors analyzed such flow with respect to an impervious object coated by a single layer of homogeneous, isotropic permeability [14–16]. In such systems, if the sphere is subjected to an axisymmetric flow, then the flow in the exterior (free-fluid) domain is characterized by exactly two coefficients, indicating that there are two components of wake [13]. That there are only two such numbers is a pure consequence of the spherical symmetry of the system, and this statement remains valid when the permeability distribution is radially inhomogeneous, or even uniaxially anisotropic, provided that the diagonal basis vectors of permeability are aligned with the spherical coordinate basis vectors everywhere. In Ref. [17], it is shown that it is possible to simultaneously null both of these wake coefficients, if permeability has a certain distribution that contains negative values, whose significance is that the solid produces volumetric thrust (acceleration). A mentioned example of a candidate material that may provide the volumetric thrust in an active hydrodynamic metamaterial is an array of active micropumps [18–21]. A negative-permeability structure was named an active hydrodynamic metamaterial (AHM); here, to describe media that contain no thrust-generating active elements we also use the name passive hydrodynamic metamaterials, or PHM. Reference [17] presented only a single, numerical and approximate solution, leaving out important questions, such

*patrick.bowen@duke.edu

 ©2015 American Physical Society

as (a) to what extent the wake coefficients can be controlled with a passive medium and (b) how can one control each of the two wake coefficients individually, rather than nulling both of them simultaneously.

We address these and other questions analytically in the Stokes limit for the class of spherically-symmetric, possibly anisotropic, permeable structures with essentially arbitrary radial permeability distributions. Our approach to a general radially-graded permeability map is to stratify it into a series of concentric layers, such that permeability in each of them can be treated as constant. Stokes flow through a homogeneous permeability layer has analytical solutions, which, in some cases, involve special functions. We show, however, that these special functions are well-known standard functions, which have been available in several industry-standard numerical and symbolic computation packages for at least a decade.

Our approach is inspired by the transfer matrix formalism used in electromagnetics to describe wave propagation through multiple homogeneous layers. Such formalism was used to determine reflection and transmission coefficients in planar geometries, and scattering coefficients in cylindrical and spherical geometries, the latter known as Mie theory [22–24]. In this formalism, the unknown fields are first expanded in each layer in the basis of general solutions to the master partial differential equation (PDE), such as the Helmholtz equation in optics, or the Brinkman-Stokes equation in our case. The field continuity conditions [25] are then used to generate a sequence of linear relations between the unknown magnitudes of the basis solutions in each layer. Finally, one constructs a combined transfer matrix relating these magnitudes in the exterior domain with those in the core domain (the spherical domain containing the geometric center of the structure), similar to the transfer matrices used in optics [26,27]. The dimension of this matrix is equal to the order of the master PDE, which, in our case, is 4. The boundary conditions at infinity and at the origin, which stem from the requirement of field and energy finiteness, are then used to express the unknown coefficients through the magnitude of the incident field, i.e., the velocity of the plug flow in the hydrodynamic case. This strategy is very similar to the calculation of the scattering coefficients in electromagnetics [28] and fluid acoustics, and it can be generalized to scattering theories that deal with either higher-rank tensor fields, such as elastodynamics and gravitational wave theory, or with higher-order PDEs, such as nonlocal wave theories.

II. STOKES FLOW IN SPHERICAL PERMEABLE STRUCTURES

As was stated, the strategy that we employ to solve the multilayer sphere problem is inspired by Mie theory in electromagnetics. This process begins by first finding the fundamental solutions to the stationary Brinkman equation in spherical coordinates and in a material with constant permeability. The flow in each layer of the multilayer sphere will then be expanded in terms of these fundamental solutions, and the boundary conditions of the problem will be used to set up a matrix equation that solves for the coefficients. We therefore begin by considering the Brinkman equation for Stokes flow through a uniform permeable medium,

$$\tilde{\mu}\nabla^2\mathbf{u} - \frac{\mu}{k}\mathbf{u} = \nabla p, \tag{1}$$

where μ is the viscosity, $\tilde{\mu}$ is the effective viscosity in the medium, and k is the permeability. The problem at hand is assumed to be axisymmetric, and therefore all quantities are functions only of the radial coordinate r and the polar angle θ. Expanding the vector Laplacian, this equation can be reexpressed as

$$\tilde{\mu}\nabla(\nabla\cdot\mathbf{u}) - \tilde{\mu}\nabla\times\nabla\times\mathbf{u} - \mu\rho\mathbf{u} = \nabla p, \tag{2}$$

where $\rho \equiv 1/k$ is the flow resistivity. Equation (1) assumes that the flow is incompressible, which results in two further simplifications. The first is that the first term in the equation above becomes zero:

$$-\tilde{\mu}\nabla\times\nabla\times\mathbf{u} - \mu\rho\mathbf{u} = \nabla p \tag{3}$$

The second simplification is that the velocity can be expressed as the curl of an arbitrary vector function, $\mathbf{u} = \nabla\times\mathbf{A}$. If the body under consideration is axisymmetric, then this vector function can be shown to have only one component [29],

$$\mathbf{A} = -\psi(r,\theta)\frac{\hat{\phi}}{r\sin(\theta)}, \tag{4}$$

where $\hat{\phi}$ is the unit azimuthal vector. This definition for the so-called Stokes's stream function has the property that

$$\nabla\times\nabla\times\left(-\psi\frac{\hat{\phi}}{r\sin(\theta)}\right) = \frac{\hat{\phi}}{r\sin(\theta)}E^2\psi, \tag{5}$$

where the operator E^2 is given by

$$E^2 = \frac{\partial^2}{\partial r^2} + \frac{\sin(\theta)}{r^2}\frac{\partial}{\partial\theta}\left(\frac{1}{\sin(\theta)}\frac{\partial}{\partial\theta}\right). \tag{6}$$

The pressure term in Stokes's equations may be eliminated by taking the curl of both sides, and applying the identity that the curl of the gradient of a scalar function is zero. Therefore, for spherical flow problems, the stream function follows the differential equation

$$E^2(E^2 - \tilde{\rho})\psi = 0 \tag{7}$$

in a domain where the permeability and effective viscosity are constant, and the variable $\tilde{\rho} = \rho\mu/\tilde{\mu}$ has been used for the effective flow resistivity. The equation is fourth order with respect to the polar angle, so there are four fundamental angular solutions. However, the only solution that satisfies the boundary conditions of plug flow at infinity is $\sin^2(\theta)$. Therefore the general solution for the stream function has the form

$$\psi(r,\theta) = \frac{U_\infty}{2}a^2\sin^2(\theta)\sum_i A_i\psi_i(r), \tag{8}$$

where a is the inner diameter of the permeable layer, and the radial basis functions $\psi_i(r)$ are solutions to the ordinary differential equation

$$\left[\left(\frac{\partial^2}{\partial r^2} - 2/r\right)^2 - \tilde{\rho}\left(\frac{\partial^2}{\partial r^2} - 2/r\right)\right]\psi_i(r) = 0. \tag{9}$$

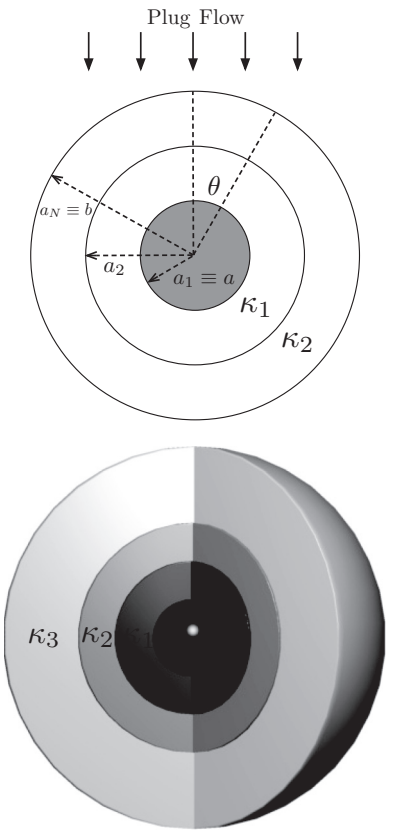

FIG. 1. Illustration of a sphere coated in multiple layers of permeable material. Each layer has permeability κ_i and inner radius a_i.

This equation is fourth order, and its fundamental solution is a linear combination of four basis functions, which are derived below.

We now consider the geometry depicted in Fig. 1: a free flow domain with $\rho = 0$ at $r > b$, and a permeable shell with radially-variable, piecewise-constant permeability in the shell $a < r < b$. In the free flow region, $\rho = 0$, and the solution is given by

$$\psi_1(r) = a/r, \tag{10a}$$
$$\psi_2(r) = (r/a), \tag{10b}$$
$$\psi_3(r) = (r/a)^2, \tag{10c}$$
$$\psi_4(r) = (r/a)^4. \tag{10d}$$

This particular normalization has been chosen so that both the basis functions and the coefficients A_i are dimensionless. When the flow resistivity is nonzero and constant, the solution is

$$\tilde{\psi}_1(r) = a/r, \tag{11a}$$
$$\tilde{\psi}_2(r) = \frac{\cosh(r\sqrt{\tilde{\rho}})}{r\sqrt{\tilde{\rho}}} - \sinh(r\sqrt{\tilde{\rho}}), \tag{11b}$$
$$\tilde{\psi}_3(r) = (r/a)^2, \tag{11c}$$
$$\tilde{\psi}_4(r) = \frac{\sinh(r\sqrt{\tilde{\rho}})}{r\sqrt{\tilde{\rho}}} - \cosh(r\sqrt{\tilde{\rho}}). \tag{11d}$$

The normalization of the permeable basis is also chosen to yield dimensionless coefficients, and shows the correspondence of $\tilde{\psi}_1(r)$ and $\tilde{\psi}_3(r)$ with $\psi_1(r)$ and $\psi_3(r)$. The last two basis functions in the free flow region, $\psi_2(r)$ and $\psi_4(r)$, can be recovered from the basis in permeable flow by forming the appropriate linear combination of the permeable basis and taking the limit as $\rho \to 0$. To find the exact correspondence between the permeable flow basis and the free flow basis, we expand each basis function in its Taylor series, create a linear combination of these basis functions that reproduces either $\psi_3(r)$ or $\psi_4(r)$, and then take the limit as $\rho \to 0$. The permeable basis functions $\tilde{\psi}_2(r)$ and $\tilde{\psi}_4(r)$ can be expressed in terms of their Taylor series as

$$\begin{aligned}\tilde{\psi}_2(r) &= \sum_{n=0}^{\infty} \frac{(\sqrt{\rho}r)^{2n-1}}{(2n)!} - \frac{(\sqrt{\rho}r)^{2n+1}}{(2n+1)!} \\ &= \frac{1}{\sqrt{\rho}r} - \sqrt{\rho}r/2 + O(\sqrt{\rho}r)^3,\end{aligned} \tag{12a}$$

$$\begin{aligned}\tilde{\psi}_4(r) &= \sum_{n=0}^{\infty} \left(\frac{-2n}{2n+1}\right) \frac{(\sqrt{\rho}r)^{2n}}{(2n)!} \\ &= -\rho r^2/3 - \rho^2 r^4/30 + O(\sqrt{\rho}r)^6.\end{aligned} \tag{12b}$$

The expansion of $\tilde{\psi}_2(r)$ only contains odd powers of r, so this function must be related to $\psi_1(r)$ and $\psi_2(r)$, while the expansion of $\tilde{\psi}_2(r)$ only contains even powers of r, so it must correspond to $\psi_3(r)$ and $\psi_4(r)$. Using this observation to guide the derivation, the limiting form of the permeable basis functions can be mapped to the free flow basis by

$$\psi_1(r) = \tilde{\psi}_1(r), \tag{13a}$$
$$\psi_2(r) = \lim_{\rho\to 0}\left(\frac{2\tilde{\psi}_1(r)}{a^2\rho} - \frac{2\tilde{\psi}_2(r)}{a\sqrt{\rho}}\right), \tag{13b}$$
$$\psi_3(r) = \tilde{\psi}_3(r), \tag{13c}$$
$$\psi_4(r) = \lim_{\rho\to 0}\left(-\frac{10\tilde{\psi}_3(r)}{a^2\rho} - \frac{30\tilde{\psi}_4(r)}{a^4\rho^2}\right). \tag{13d}$$

The singularities in each of the two terms that are involved in taking the limit cancel each other out, and the higher order terms seen in Eqs. (12a) and (12b) go to zero. The result is that the functions in Eqs. (10a) to (10d) are reproduced. From this point on in this paper, the tilde in the notation $\tilde{\psi}_i(r)$ that is used to distinguish it as a basis function for nonzero permeability will be dropped, and it will be implied from the context that if the flow is in a free flow region then the basis from Eqs. (10a) to (10d) should be chosen, while if the flow is in a permeable region then the basis from Eqs. (11a) to (11d) should be chosen.

III. DERIVATION OF FIELDS IN ISOTROPIC PERMEABILITY STRUCTURES

Solving the multilayer sphere problem requires applying the boundary conditions that the velocity and stress tensor are both continuous everywhere. In this section we derive a set of operators that, when applied to the stream function

radial basis functions, will reproduce the velocity vector field and the stress tensor field. Since the only difference between the free flow solution and the permeable solution lies in the radial basis functions, all of the expressions here will be left in terms of an operator acting on an arbitrary radial basis function.

A. Expressions for the velocity field

Expanding out the curl equation for the velocity, $\mathbf{u} = -\nabla \times (\psi(r,\theta)\frac{\hat{\phi}}{r\sin(\theta)})$, the velocity can be expressed as

$$u_r = \frac{-1}{r^2\sin(\theta)}\frac{\partial}{\partial\theta}\psi(r,\theta), \tag{14}$$

$$u_\theta = \frac{1}{r\sin(\theta)}\frac{\partial}{\partial r}\psi(r,\theta). \tag{15}$$

When the stream function in Eq. (8) is substituted into these equations, we obtain

$$u_r = U_\infty\cos(\theta)\sum_i A_i\left(\frac{-a^2}{r^2}\right)\psi_i(r), \tag{16}$$

$$u_\theta = U_\infty\sin(\theta)\sum_i A_i\left(\frac{a^2}{2r}\right)\frac{\partial}{\partial r}\psi_i(r). \tag{17}$$

B. Expressions for the pressure field

Stokes's equation can be used to relate the stream function to the gradient of the pressure:

$$\nabla\times\left(\frac{\hat{\phi}}{r\sin(\theta)}E^2\psi\right) - \tilde{\rho}\nabla\times\left(\psi\frac{\hat{\phi}}{r\sin(\theta)}\right) = -\frac{1}{\tilde{\mu}}\nabla p. \tag{18}$$

This last equation can be written out in components for the partial derivatives of the pressure:

$$\frac{\partial p}{\partial r} = -\frac{\tilde{\mu}}{r^2\sin(\theta)}\left(\frac{\partial}{\partial\theta}E^2\psi - \tilde{\rho}\frac{\partial}{\partial\theta}\psi\right), \tag{19}$$

$$\frac{\partial p}{\partial\theta} = \frac{\tilde{\mu}}{\sin(\theta)}\left(\frac{\partial}{\partial r}E^2\psi - \tilde{\rho}\frac{\partial}{\partial r}\psi\right). \tag{20}$$

Substituting the stream function in these equations, and using the property that

$$E^2\psi = \frac{1}{2}U_\infty\sin^2(\theta)\sum_i a^2A_i\left(\frac{\partial^2}{\partial r^2} - \frac{2}{r^2}\right)\psi_i \tag{21}$$

we obtain the following expressions for the derivatives of the pressure:

$$\frac{\partial p}{\partial r} = \tilde{\mu}U_\infty\cos(\theta)\sum_i A_i\left(\frac{a^2}{2}\right)\left(\frac{2}{r^2}\right)\left(\tilde{\rho} + \frac{2}{r^2} - \frac{\partial^2}{\partial r^2}\right)\psi_i(r), \tag{22a}$$

$$\frac{\partial p}{\partial\theta} = -\tilde{\mu}U_\infty\sin(\theta)\sum_i A_i\left(\frac{a^2}{2}\right)\frac{\partial}{\partial r}\left(\tilde{\rho} + \frac{2}{r^2} - \frac{\partial^2}{\partial r^2}\right)\psi_i(r). \tag{22b}$$

If the pressure is to be part of the solution of Stokes's equation, then the derivatives must satisfy an exact differential, $dp = \frac{\partial p}{\partial r}dr + \frac{\partial p}{\partial\theta}d\theta$, so that they are integrable. The condition that they form an exact differential is

$$\frac{\partial^2}{\partial r^2}\left(\tilde{\rho} + \frac{2}{r^2} - \frac{\partial^2}{\partial r^2}\right)\psi_i(r) = \left(\frac{2}{r^2}\right)\left(\tilde{\rho} + \frac{2}{r^2} - \frac{\partial^2}{\partial r^2}\right)\psi_i(r), \tag{23}$$

which is equivalent to Eq. (9), and therefore any valid stream function will render a scalar field under this operator that is integrable. The solution for the pressure is found by integrating Eq. (22b) with respect to the polar angle:

$$p = p_\infty + U_\infty\cos(\theta)\sum_i A_i\left(\tilde{\mu}\frac{a^2}{2}\right)\frac{\partial}{\partial r}\left(\tilde{\rho} + \frac{2}{r^2} - \frac{\partial^2}{\partial r^2}\right)\psi_i(r). \tag{24}$$

The pressure in free flow is then given by the same linear operator, but excluding the $\tilde{\rho}$ term:

$$p = p_\infty + \tilde{\mu}U_\infty\cos(\theta)\sum_i A_i\left(\frac{a^2}{2}\right)\frac{\partial}{\partial r}\left(\frac{2}{r^2} - \frac{\partial^2}{\partial r^2}\right)\psi_i(r). \tag{25}$$

C. Stress tensor in isotropic, spherically-symmetric systems

The stress tensor is most commonly computed using the pressure and derivatives of the velocity. The velocity in any permeable material is related to the stream function in the same way that it is related to the stream function when it is in free space, and this relationship is given in Eqs. (16) and (17). However, the operator that defines the relationship between the stream function and the pressure depends on the permeability of the medium.

In the permeable layer, the components of the stress tensor are

$$T_{rr} = -p + 2\tilde{\mu}\frac{\partial}{\partial r}u_r, \tag{26}$$

$$T_{r\theta} = \tilde{\mu}\frac{1}{r}\frac{\partial}{\partial\theta}u_r + \tilde{\mu}\left(\frac{\partial}{\partial r} - \frac{1}{r}\right)u_\theta. \tag{27}$$

Substituting the equations for the velocity, these become

$$T_{rr} = U_\infty\cos(\theta)\sum_i A_i(\tilde{\mu}a^2/2)\left(\frac{\partial^3}{\partial r^3} - \frac{\partial}{\partial r}\frac{6}{r^2} - \tilde{\rho}\frac{\partial}{\partial r}\right)\psi_i, \tag{28}$$

$$T_{r\theta} = U_\infty\sin(\theta)\sum_i A_i(\tilde{\mu}a^2/2)\left(\frac{2}{r^3} - \frac{2}{r^2}\frac{\partial}{\partial r} + \frac{1}{r}\frac{\partial^2}{\partial r^2}\right)\psi_i. \tag{29}$$

These become the equations for the stress tensor in a free flow regime in the limit of infinite permeability.

IV. THE CASE WITH ANISOTROPIC-PERMEABILITY LAYERS

In Sec. II, the Brinkman equation was presented with an isotropic permeability. The total solution space may be

expanded by allowing this permeability to anisotropic. The Brinkman equation may be more conveniently rewritten in terms of the flow resistivity instead of the permeability, where the flow resistivity is allowed to be a tensor:

$$\nabla \times \nabla \times \mathbf{u} + \tilde{\rho}\mathbf{u} = -\frac{1}{\tilde{\mu}}\nabla p. \tag{30}$$

Because we assume spherical symmetry, only the radial and azimuthal components of the resistivity are allowed to be nonzero, which we shall see immediately below. Following the approach that was taken Sec. II, the stream function form of the vector potential is substituted for the velocity and the curl is taken of both sides to remove the pressure dependence:

$$\nabla \times \nabla \times \nabla \times \nabla \times \frac{-\psi(r,\theta)}{r\sin(\theta)}\hat{\theta} + \nabla \times \left(\tilde{\rho}\nabla \times \frac{-\psi(r,\theta)}{r\sin(\theta)}\right) = 0. \tag{31}$$

The first term on the left reduces to a repeated operator of E^2 in the usual way,

$$\frac{-\hat{\theta}}{r\sin(\theta)}E^4\psi + \nabla \times \left(\tilde{\rho}\nabla \times \frac{-\psi(r,\theta)}{r\sin(\theta)}\right) = 0, \tag{32}$$

but the term on the right cannot be reduced in the same way because the resistivity matrix is no longer a spherical tensor. Instead, we obtain

$$\nabla \times \left(\tilde{\rho}\nabla \times \frac{-\psi(r,\theta)}{r\sin(\theta)}\right) = \frac{\hat{\theta}}{r\sin(\theta)}\left[\tilde{\rho}_{rr}E^2 + (\tilde{\rho}_{\theta\theta}-\tilde{\rho}_{rr})\frac{\partial^2}{\partial r^2} - \tilde{\rho}_{r\theta}L\right]\psi(r,\theta), \tag{33}$$

where

$$L = \frac{\sin(\theta)+1}{r\sin^2(\theta)}\frac{\partial}{\partial\theta}\frac{\partial}{\partial r} - \frac{1}{r^2}\frac{\partial}{\partial\theta}. \tag{34}$$

Putting these equations together, the stream function is now a solution to the differential equation

$$\left(E^4 - \tilde{\rho}_{rr}E^2 - (\tilde{\rho}_{\theta\theta} - \tilde{\rho}_{rr})\frac{\partial^2}{\partial r^2} + \tilde{\rho}_{r\theta}L\right)\psi(r,\theta) = 0. \tag{35}$$

If the off-diagonal elements remain zero such that the principal eigenvectors of the resistivity matrix preserve the symmetry of the system, then the L operator drops out. The angular dependence is then unperturbed, and $\sin^2(\theta)$ remain a separable solution. In what follows, we assume that $\rho = \mathrm{diag}(\rho_r \equiv \rho_{rr}, \rho_\theta \equiv \rho_{\theta\theta})$. The four radial basis functions, $\psi_i(r)$, must satisfy the fourth-order ordinary differential equation

$$\left(\left(\frac{\partial^2}{\partial r^2} - 2/r^2\right)^2 + 2\tilde{\rho}_r/r^2 - \tilde{\rho}_\theta\frac{\partial^2}{\partial_r^2}\right)\psi_i(r) = 0. \tag{36}$$

The solutions to this equation are

$$\psi_1(r) = r\sqrt{\tilde{\rho}_\theta}F_{2,3}\left(\left\{1/4 - \frac{\sqrt{8\tilde{\rho}_r+\tilde{\rho}_\theta}}{4\sqrt{\tilde{\rho}_\theta}}, 1/4 + \frac{\sqrt{8\tilde{\rho}_r+\tilde{\rho}_\theta}}{4\sqrt{\tilde{\rho}_\theta}}\right\}, \{-1/2,1/2,2\}, r^2\tilde{\rho}_\theta/4\right), \tag{37a}$$

$$\psi_2(r) = r^4\tilde{\rho}_\theta^2F_{2,3}\left(\left\{7/4 - \frac{\sqrt{8\tilde{\rho}_r+\tilde{\rho}_\theta}}{4\sqrt{\tilde{\rho}_\theta}}, 7/4 + \frac{\sqrt{8\tilde{\rho}_r+\tilde{\rho}_\theta}}{4\sqrt{\tilde{\rho}_\theta}}\right\}, \{2,5/2,7/2\}, r^2\tilde{\rho}_\theta/4\right), \tag{37b}$$

$$\psi_3(r) = G_{2,4}^{2,2}\left(\left\{\left[5/4 - \frac{\sqrt{8\tilde{\rho}_r+\tilde{\rho}_\theta}}{4\sqrt{\tilde{\rho}_\theta}}, 5/4 + \frac{\sqrt{8\tilde{\rho}_r+\tilde{\rho}_\theta}}{4\sqrt{\tilde{\rho}_\theta}}\right], [\,]\right\}, \{[-1/2,1/2],[1,2]\}, r^2\tilde{\rho}_\theta/4\right), \tag{37c}$$

$$\psi_4(r) = G_{2,4}^{2,2}\left(\left\{\left[5/4 - \frac{\sqrt{8\tilde{\rho}_r+\tilde{\rho}_\theta}}{4\sqrt{\tilde{\rho}_\theta}}, 5/4 + \frac{\sqrt{8\tilde{\rho}_r+\tilde{\rho}_\theta}}{4\sqrt{\tilde{\rho}_\theta}}\right], [\,]\right\}, \{[1,2],[-1/2,1/2]\}, r^2\tilde{\rho}_\theta/4\right), \tag{37d}$$

where F is the hypergeometric function and G is the Meijer G function.

A. Stress tensor in anisotropic spherically-symmetric systems

In the case of anisotropic permeability, the operator that relates the pressure to the stream function can be expressed in terms of only one component of the permeability tensor. In this section the operator is derived explicitly in terms of the polar component of the flow resistivity tensor, since the approach using that component is somewhat simpler.

Once the solution for the stream function has been found, the derivatives of the pressure can be extracted from Stokes's equation:

$$\frac{\partial p}{\partial r} = -\frac{\tilde{\mu}}{r^2\sin(\theta)}\left(\frac{\partial}{\partial\theta}E^2\psi - \tilde{\rho}_r\frac{\partial}{\partial\theta}\psi\right), \tag{38a}$$

$$\frac{\partial p}{\partial\theta} = \frac{\tilde{\mu}}{\sin(\theta)}\left(\frac{\partial}{\partial r}E^2\psi - \tilde{\rho}_\theta\frac{\partial}{\partial r}\psi\right). \tag{38b}$$

Given that the angular solution is $\sin^2(\theta)$, the derivatives of pressure can be expressed solely in terms of radial derivatives of the radial basis functions:

$$\frac{\partial p}{\partial r} = \tilde{\mu}U_\infty\cos(\theta)\sum_i A_i\left(\frac{a^2}{2}\right)\left(\frac{2}{r^2}\right)\left(\tilde{\rho}_r + \frac{2}{r^2} - \frac{\partial^2}{\partial r^2}\right)\psi_i(r), \tag{39a}$$

$$\frac{\partial p}{\partial\theta} = -\tilde{\mu}U_\infty\sin(\theta)\sum_i A_i\left(\frac{a^2}{2}\right)\left(\frac{\partial}{\partial r}\right)\left(\tilde{\rho}_\theta + \frac{2}{r^2} - \frac{\partial^2}{\partial r^2}\right)\psi_i(r). \tag{39b}$$

The condition that these equations be integrable is

$$\left(\frac{2}{r^2}\right)\left(\tilde{\rho}_r + \frac{2}{r^2} - \frac{\partial^2}{\partial r^2}\right)\psi_i(r) = \left(\frac{\partial^2}{\partial r^2}\right)\left(\tilde{\rho}_\theta + \frac{2}{r^2} - \frac{\partial^2}{\partial r^2}\right)\psi_i(r), \tag{40}$$

which is equivalent to Eq. (36), just as in the isotropic case. The pressure is found by integrating Eq. (39b) with respect to the polar angle:

$$p = p_\infty + \tilde{\mu} U_\infty \cos(\theta) \sum_i A_i \left(\frac{a^2}{2}\right)\left(\frac{\partial}{\partial r}\right) \times \left(\tilde{\rho}_\theta + \frac{2}{r^2} - \frac{\partial^2}{\partial r^2}\right)\psi_i(r). \tag{41}$$

The stress tensor is therefore

$$T_{rr} = U_\infty \cos(\theta) \sum_i A_i (\tilde{\mu} a^2/2)\left(\frac{\partial^3}{\partial r^3} - \frac{\partial}{\partial r}\frac{6}{r^2} - \tilde{\rho}_\theta \frac{\partial}{\partial r}\right)\psi_i, \tag{42}$$

$$T_{r\theta} = U_\infty \sin(\theta) \sum_i A_i (\tilde{\mu} a^2/2)\left(\frac{2}{r^3} - \frac{2}{r^2}\frac{\partial}{\partial r} + \frac{1}{r}\frac{\partial^2}{\partial r^2}\right)\psi_i. \tag{43}$$

V. ALGORITHM FOR SOLVING THE MULTILAYER PROBLEM

One unique aspect of Mie theory problems is the arrangement of the boundary conditions. For an Mth order differential equation there will be M linearly independent solutions in each of the domains, which correspond to M unknown coefficients for each of these solutions in each layer of the system. Then there will be M boundary conditions relating each layer to its adjacent layer in either direction. For a problem with N domains there will be $N-1$ interfaces between the domains, so only $N-1$ sets of M equations. These boundary conditions allow the interior domains to be connected in such a way that the coefficients of the basis functions in the outermost domain are related to the coefficients of the innermost domain by a linear map. The final M equations needed to solve the problem are given by the boundary conditions for the global problem. In this particular case, $M = 4$, and there are two boundary conditions on the innermost spherical shell and two boundary conditions on the limiting form of the free flow region, which is the final domain. The challenge is to arrange the problem so that these two sets of two boundary conditions can be combined together to provide a final set of M equations that allow the entire problem to be solved. Stokes's stream function here assumes a piecewise form, $\psi(r) = \sum_{i=1}^4 A_i^j \psi_i^j(r)$, $a_j < r < a_{j+1}$, $j = 1, \ldots, N$, where the $\psi_i^j(r)$ in each layer are given by

$$\tilde{\psi}_1^j(r) = a_j/r, \tag{44a}$$

$$\tilde{\psi}_2^j(r) = \frac{\cosh(r\sqrt{\tilde{\rho}_j})}{r\sqrt{\tilde{\rho}_j}} - \sinh(r\sqrt{\tilde{\rho}_j}), \tag{44b}$$

$$\tilde{\psi}_3^j(r) = (r/a_j)^2, \tag{44c}$$

$$\tilde{\psi}_4^j(r) = \frac{\sinh(r\sqrt{\tilde{\rho}_j})}{r\sqrt{\tilde{\rho}_j}} - \cosh(r\sqrt{\tilde{\rho}_j}) \tag{44d}$$

in the permeable layers and

$$\psi_1^j(r) = y a_j/r, \tag{45a}$$

$$\psi_2^j(r) = (r/a_j), \tag{45b}$$

$$\psi_3^j(r) = (r/a_j)^2, \tag{45c}$$

$$\psi_4^j(r) = (r/a_j)^4 \tag{45d}$$

in the free-flow domain, which is when $j = N$.

For the interfaces between the domains, the boundary conditions are that velocity must be continuous, and the components of the stress tensor must also be continuous. At the outer radius of the jth layer, $r = a_{j+1}$, this means that

$$\sum_i A_i^j L_{rr}^j \psi_i^j(a_{j+1}) = \sum_i A_i^{j+1} L_{rr}^{j+1} \psi_i^{j+1}(a_{j+1}), \tag{46}$$

$$\sum_i A_i^j L_{r\theta}^j \psi_i^j(a_{j+1}) = \sum_i A_i^{j+1} L_{r\theta}^{j+1} \psi_i^{j+1}(a_{j+1}), \tag{47}$$

$$\sum_i A_i^j L_r^j \psi_i^j(a_{j+1}) = \sum_i A_i^{j+1} L_r^{j+1} \psi_i^{j+1}(a_{j+1}), \tag{48}$$

$$\sum_i A_i^j L_\theta^j \psi_i^j(a_{j+1}) = \sum_i A_i^{j+1} L_\theta^{j+1} \psi_i^{j+1}(a_{j+1}), \tag{49}$$

where

$$L_{rr}^j = (\tilde{\mu}_j a_j^2/2)\left(\frac{\partial^3}{\partial r^3} - \frac{\partial}{\partial r}\frac{6}{r^2} - \tilde{\rho}_\theta \frac{\partial}{\partial r}\right), \tag{50}$$

$$L_{r\theta}^j = (\tilde{\mu}_j a_j^2/2)\left(\frac{2}{r^3} - \frac{2}{r^2}\frac{\partial}{\partial r} + \frac{1}{r}\frac{\partial^2}{\partial r^2}\right) \tag{51}$$

are linear operators that transform the stream function in the jth layer into components of the stress tensor, and

$$L_r^j = \frac{-a_j^2}{r^2}, \tag{52}$$

$$L_\theta^j = \left(\frac{a_j^2}{2r}\right)\frac{\partial}{\partial r} \tag{53}$$

are linear operators that transform the stream function in the jth layer into velocity components. Using these linear operators, the continuity boundary conditions can be expressed in a matrix form

$$\mathbf{A}^j = \mathbf{M}^{j+1}\mathbf{A}^{j+1}, \tag{54}$$

where

$$\mathbf{M}^{j+1} = (\mathbf{S}^j(a_{j+1}))^{-1}(\mathbf{S}^{j+1}(a_{j+1})), \tag{55}$$

$$\mathbf{S}^j(a) = \begin{bmatrix} L_r^j\psi_1^j|_a & L_r^j\psi_2^j|_a & L_r^j\psi_3^j|_a & L_r^j\psi_4^j|_a \\ L_\theta^j\psi_1^j|_a & L_\theta^j\psi_2^j|_a & L_\theta^j\psi_3^j|_a & L_\theta^j\psi_4^j|_a \\ L_{rr}^j\psi_1^j|_a & L_{rr}^j\psi_2^j|_a & L_{rr}^j\psi_3^j|_a & L_{rr}^j\psi_4^j|_a \\ L_{r\theta}^j\psi_1^j|_a & L_{r\theta}^j\psi_2^j|_a & L_{r\theta}^j\psi_3^j|_a & L_{r\theta}^j\psi_4^j|_a \end{bmatrix}, \tag{56}$$

and $\mathbf{A}^j = [A_1^j A_2^j A_3^j A_4^j]^t$ is a vector containing the coefficients for the jth layer. The coefficients in the outermost layer can be

consequently expressed as a linear function of the coefficients of the the innermost layer.

The boundary condition on the innermost layer is that the velocity goes to zero. This can be expressed as the matrix equation

$$\mathbf{b}_{in} = \begin{bmatrix} 0 \\ 0 \end{bmatrix} \tag{57}$$

$$= \begin{bmatrix} L_r^1\psi_1^1|_{a_1} & L_r^1\psi_2^1|_{a_1} & L_r^1\psi_3^1|_{a_1} & L_r^1\psi_4^1|_{a_1} \\ L_\theta^1\psi_1^1|_{a_1} & L_\theta^1\psi_2^1|_{a_1} & L_\theta^1\psi_3^1|_{a_1} & L_\theta^1\psi_4^1|_{a_1} \end{bmatrix} \begin{bmatrix} A_1^1 \\ A_2^1 \\ A_3^1 \\ A_4^1 \end{bmatrix} \tag{58}$$

or

$$\mathbf{b}_{in} = \mathbf{B}_{in}\mathbf{A}^1. \tag{59}$$

The boundary condition on the outermost layer requires that

$$\lim_{r\to\infty} u_r = -U_\infty \cos(\theta), \tag{60}$$

$$\lim_{r\to\infty} u_\theta = U_\infty \sin(\theta). \tag{61}$$

Combined with Eqs. (16) and (17), this boundary condition at infinity implies that $A_3^N = -1$ and $A_4^N = 0$. This can also be expressed in a matrix equation

$$\mathbf{b}_{out} = \mathbf{B}_{out}\mathbf{A}^N, \tag{62}$$

where

$$\mathbf{B}_{out} = \begin{bmatrix} 0 & 0 & 1 & 0 \\ 0 & 0 & 0 & 1 \end{bmatrix} \tag{63}$$

and

$$\mathbf{b}_{out} = \begin{bmatrix} -1 \\ 0 \end{bmatrix} \tag{64}$$

and $\mathbf{A}^N$ are the coefficients in the free flow domain. These boundary conditions can be combined by first recognizing that $\mathbf{A}^1 = (\prod_{j=2}^N \mathbf{M}^j)\mathbf{A}^N \equiv \mathbf{M}_T\mathbf{A}^N$. Then the entire system can be expressed in the block matrix form

$$\begin{bmatrix} \mathbf{b_{in}} \\ \mathbf{b}_{out} \end{bmatrix} = \begin{bmatrix} \mathbf{B_{in}M_T} \\ \mathbf{B}_{out} \end{bmatrix} \mathbf{A}^N. \tag{65}$$

This is a linear problem of size and rank 4, regardless of the number of layers, which could be solved to yield the four coefficients in the exterior domain. However, since the final two components of $\mathbf{A}_N$, namely (A_3^N, A_4^N), are known to be $(-1,0)$, we can simplify this equation to a system of rank 2. The top two rows of the matrix equation may be expanded according to

$$\mathbf{b}_{in} = \mathbf{B}_{in}\mathbf{M}_{TR}\begin{bmatrix} A_1^N \\ A_2^N \end{bmatrix} - \mathbf{B}_{in}\mathbf{V}_T, \tag{66}$$

where

$$\mathbf{M}_{TR} = \begin{bmatrix} M_{T11} & M_{T21} & M_{T31} & M_{T41} \\ M_{T12} & M_{T22} & M_{T32} & M_{T42} \end{bmatrix}^t \tag{67}$$

and

$$\mathbf{V}_T = [M_{T13} \quad M_{T23} \quad M_{T33} \quad M_{T43}]^t. \tag{68}$$

Then the equation becomes a 2×2 matrix equation that can be easily inverted to solve for the coefficients A_1^N, A_2^N in the exterior domain:

$$\mathbf{B}_{in}\mathbf{M}_{TR}\begin{bmatrix} A_1^N \\ A_2^N \end{bmatrix} = \mathbf{B}_{in}\mathbf{V}_T. \tag{69}$$

VI. RESULTS

The primary quantities of interest in this paper are the wake and drag of the spherical structure. The drag force F_D is proportional to the A_2 coefficient in the exterior domain, which is more commonly referred to in the literature [13] as the B coefficient. The drag force is given by

$$F_D = 4\mu U_\infty b B, \tag{70}$$

where b is the outermost radius of the structure.

There are many possible ways in which the wake may be defined, but in this work we define it as the surface integral over a sphere centered at the multilayer structure of the deviation of the velocity from the incident plug flow at some radius r_e:

$$W = \frac{1}{U_\infty^2}\oint_{r=r_e} |\mathbf{u} - U_\infty\hat{\mathbf{z}}|^2 d\Omega. \tag{71}$$

Using the basis of free flow in the exterior domain in Eqs. (10a) to (10d), the wake can be expressed solely in terms of the coefficients in the exterior domain,

$$W = 2\pi\left(\left(b^6/r_e^6\right)A^2 + \left(b^2/r_e^2\right)B^2 + (2/3)\left(b^4/r_e^4\right)AB\right), \tag{72}$$

where we have defined $A = A_1$ and $B = A_2$ to be consistent with previously established notation in the literature [13]. We choose the evaluation radius to be the outer radius of the multilayer sphere so that $r_e = b$, and the wake becomes a simple quadratic form in A and B,

$$W = 2\pi(A^2 + B^2 + (2/3)AB). \tag{73}$$

The wake and drag may be converted into units that are comparable to one another by defining the effective radius with respect to the drag force R_D, and the effective radius with respect to the wake R_W. We define the effective radius with respect to drag or wake of a multilayer permeable structure as the radius that a solid sphere would have to take in order to reproduce the same drag or wake as the multilayer structure, respectively. To define these quantities, we evaluate Eqs. (70) and (72) using the coefficients (A_1, A_2, A_3, A_4) for a solid sphere. These equations therefore establish a fixed relationship between drag force (or wake) with the radius b required by the solid sphere to produce that drag force (or wake). This outer radius b is therefore the equivalent radius with respect to drag R_D if it is computing using the drag force in Eq. (70), or it is the equivalent radius with respect to wake R_W if it is computed using Eq. (72). For a solid sphere, the coefficients in the exterior domain are given by $(A_1, A_2, A_3, A_4) = (A, B, C, D) = (-1/2, 3/2, -1, 0)$. If these are inserted into Eq. (70), then Eq. (70) may be inverted to solve for $b \equiv R_D$ in terms of the drag force (and hence the B coefficient) of the multilayer structure. Similarly, the coefficients for a solid sphere may be inserted into Eq. (72), and Eq. (72) may be inverted to solve for $b \equiv R_W$ in terms of the wake of the multilayer structure. The effective radius with

respect to drag is then

$$R_D = 2bB/3 \tag{74}$$

and the effective radius with respect to wake is

$$R_W = b\left(2/3 + \frac{23\pi^{1/3}}{3\xi^{1/3}} - \left(\frac{\xi}{9\pi}\right)^{1/3}\right)^{1/2}, \tag{75}$$

where

$$\xi = 73\pi - 27W + 3\sqrt{3}\sqrt{648\pi^2 - 146\pi W + 27W^2}. \tag{76}$$

A. Wake control with passive structures

In order to explore the degree to which the wake and drag of a sphere of radius a might be controlled using a multilayer structure with outer radius b, we select a fixed number of layers N of permeable material of equal thickness that lie between the radii a and b. Then we employ a Monte -Carlo technique to explore the solution space by randomly selecting a large number ($\approx 5 \times 10^4$) of N-dimensional vectors $\mathbf{k} = (k_1, k_2, \ldots, k_N)$ that represent the permeability values for each of the layers in the multilayer sphere. The values of permeability components k_i were uniformly distributed on a logarithmic scale within the interval from $k_i/a^2 = 10^{-1}$ to $k_i/a^2 = 10^3$, since this range appears to provide both a good sampling of the manifold and good numerical stability. The resulting equivalent radii with respect to wake and drag of each solution is then plotted, depicting a cloud of points that demonstrate the range of wake and drag values that can be achieved if the sphere is coated with N layers of permeable material.

In Fig. 2(a), an aspect ratio b/a of 5 was chosen between the outermost radius and innermost radius ($b = 5$), and the number of layers was steadily increased while the flow resistivity was required to be isotropic. As expected, the range of possible wake and drag values converges to a smooth manifold as the number of layers increases, which demonstrates the range of physically possible wake and drag values if the flow resistivity was allowed to vary continuously with radius. Based on Fig. 2(c), the aspect ratio itself is observed to simply scale this manifold linearly.

For an anisotropic structure, a single layer of permeable material has two degrees of freedom, and therefore it results in a two-dimensional manifold as shown in Fig. 3(a). The lower boundary of this manifold appears to coincide perfectly with the lower boundary of the two-layer isotropic structure, but the upper portion of the double layer isotropic structure is unreachable by the single layer anisotropic structure. It appears that the single layer anisotropic structure behaves in some way like a double layer isotropic structure, but is not able to completely reproduce its range of wake and drag control. However, Fig. 3(b) shows that the manifold wake and drag values for a single layer anisotropic structure are greatly enlarged by the addition of more layers.

Although these results do appear to show that the drag force and wake are tightly correlated, the permeable layers are able to reduce the wake and drag. This finding is in agreement with [14], which showed that the drag force on a permeable sphere is equivalent to the drag on an impermeable sphere of reduced radius.

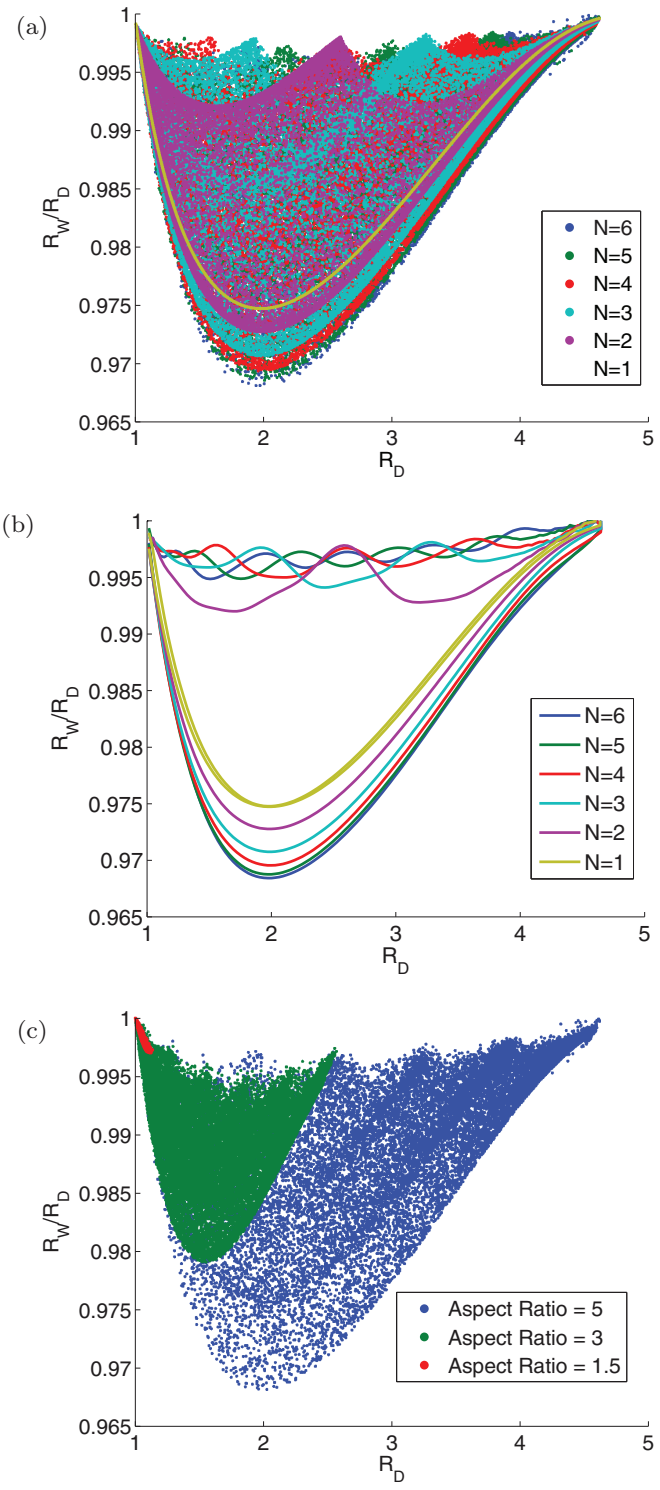

FIG. 2. (Color) (a) Convergence of the range of possible wake and drag values as the number of layers of permeable material N increases for a multilayer structure of isotropic permeable layers, for a multilayer structure with $b/a = 5$. (b) A sketch of the outline of the manifolds shown in (a) as N varies. The solution space converges as N increases. (c) Variation of the solution space as the aspect ratio b/a of the multilayer structure increases, when $N = 6$. Note that, for an impermeable sphere of radius $a \leqslant R \leqslant b$, we have $R_W = R_D = R$, which corresponds to a horizontal straight line where $R_W/R_D = 1$.

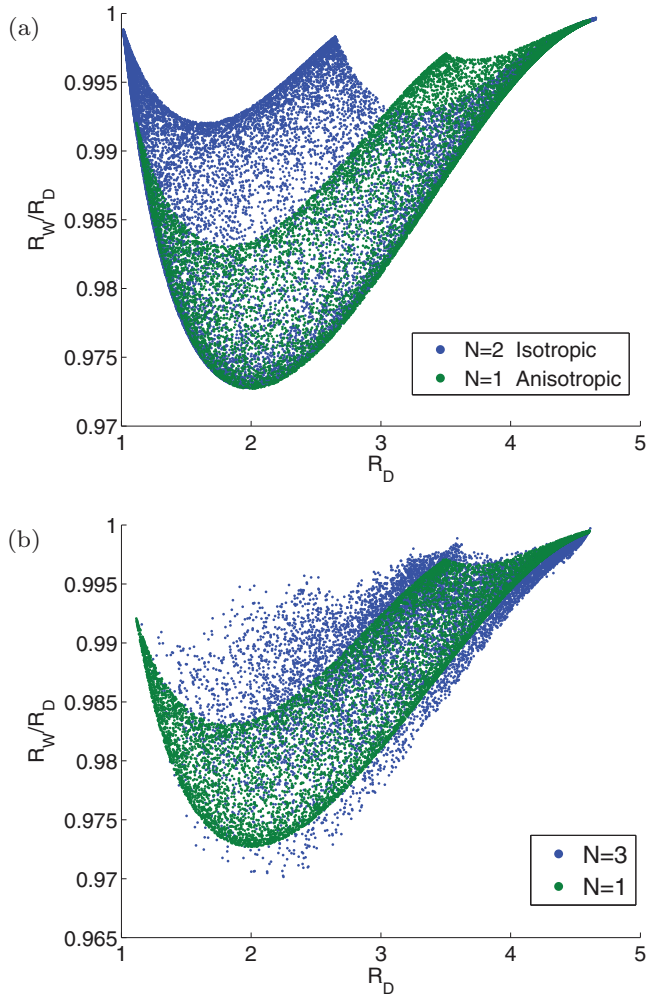

FIG. 3. (Color) (a) Comparison of the solution space of R_W/R_D and R_D values for a single layer of anisotropic material with the solution space for two layers of isotropic material, in the case where $b/a = 5$. (b) Variation of the solution space of as number of anisotropic layers increases.

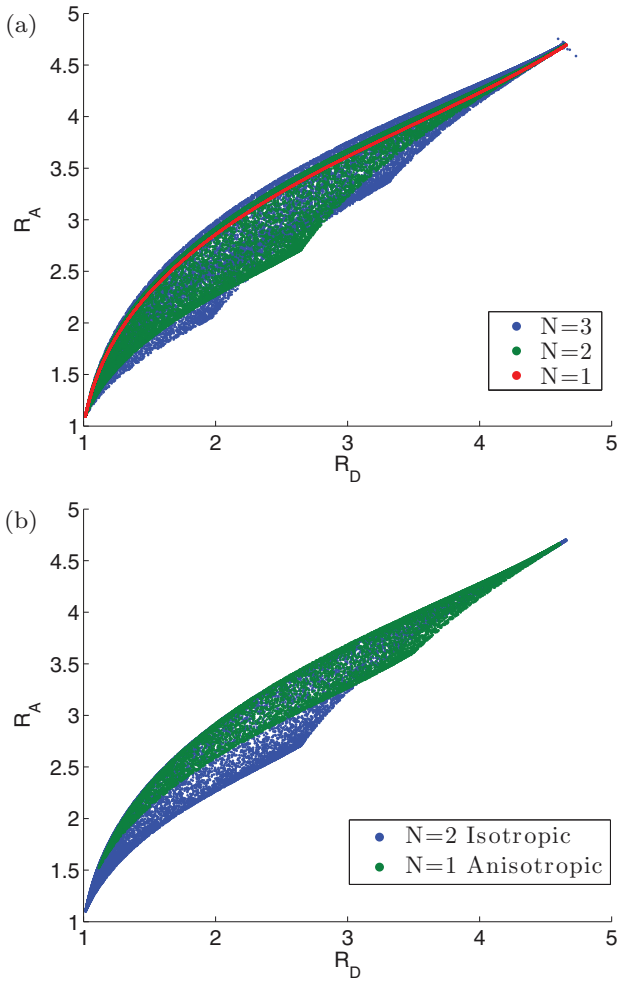

FIG. 4. (Color) (a) Convergence of the range of possible R_A and R_D values as the number of layers N of isotropic permeable material increases, when $b/a = 5$. (b) Comparison of the range of possible R_A and R_D values for a single layer of anisotropic material with the solution space for two layers of isotropic material. For an impermeable sphere of radius $a \leqslant R \leqslant b$, the solution space is $R_A = R_D = R$, which corresponds to a diagonal line from $R_A = R_D = 1$ to $R_A = R_D = 5$.

The effective radius with respect to drag only depends on the B coefficient, and therefore it is well quantified by R_D. A way to quantify the effect of the multilayer structure on the A coefficient independently of the B coefficient is to use the equivalent radius with respect to the A coefficient, R_A, where $A = A_1$ in the exterior domain. The effective radius with respect to the A coefficient is defined as the radius that an impermeable sphere would have to take in order to reproduce the same A coefficient that is created by the multilayer sphere structure. This definition implies that

$$R_A = -\mathrm{sgn}(A)b(2|A|)^{1/3}. \tag{77}$$

The range of possible R_A values versus R_D is then a measure of the degree of control that is available for the A coefficient for a given B coefficient, or drag force. This range is shown based on a Monte Carlo study in Fig. 4(a), where a considerable degree of control of R_A is shown for as few as two or three layers.

B. Wake and drag cancellation with active metamaterials

A multilayer structure with active flow resistivity is one that allows the flow resistivity to be less than zero. Since a positive, isotropic flow resistivity is defined as the application of a volumetric force in the direction opposite the flow velocity, a negative, isotropic flow resistivity is the application of a volumetric force parallel to the flow velocity. This necessarily entails pumping energy into the system, and allowing the flow resistivity to be negative therefore gives a much larger range of wake and drag control, in addition to providing interesting propulsive solutions where the drag is negative and cloaking solutions where both the wake and drag are zero.

If we begin with a six-layer isotropic multilayer structure with an aspect ratio of $b/a = 5$, and slowly increase the allowed volumetric force, then the wake to drag ratio significantly increases as the drag force decreases, as shown in Fig. 5(a). The ratio then decreases again as the drag force

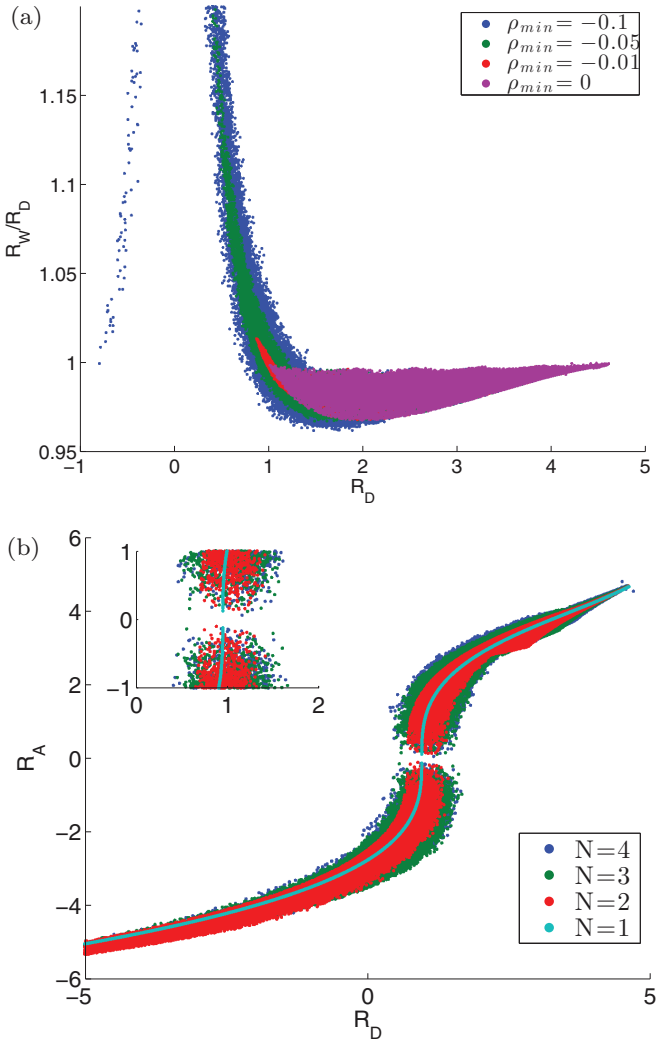

FIG. 5. (Color) (a) Convergence of the range of possible wake and drag values as the minimum allowed flow resistivity is varied, given a six-layer multilayer structure with an aspect ratio of $b/a = 5$. (b) Convergence of the effective radius with respect to the A coefficient as the number of layers is increased.

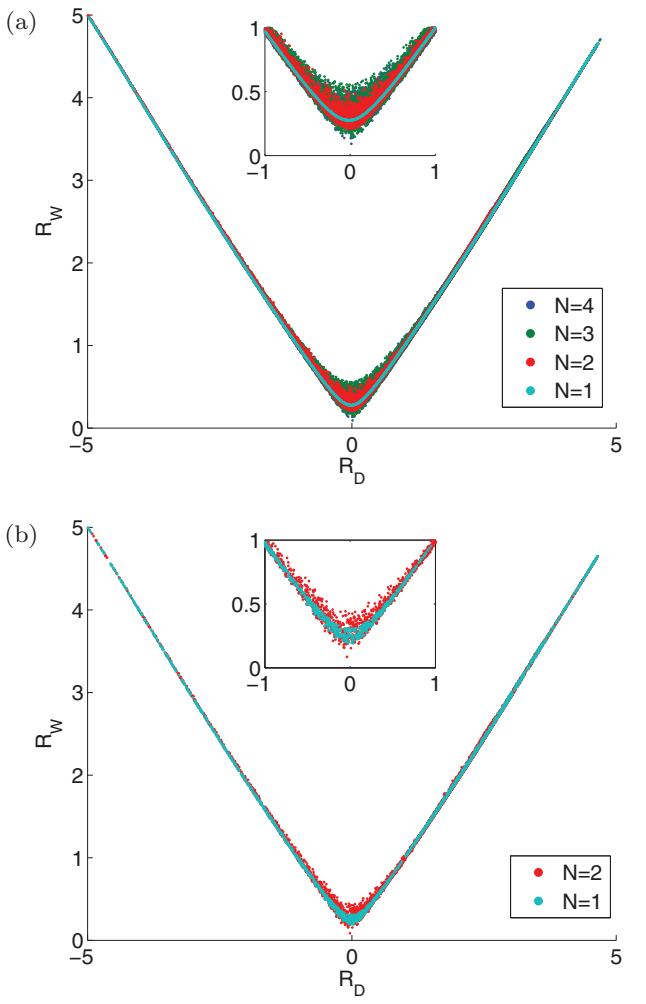

FIG. 6. (Color) Range of possible wake and drag values for active isotropic (a) and anisotropic (b) layers.

becomes negative and the structure is propelled through the liquid.

Figure 5(b) shows the degree to which R_A and R_D may be controlled independently using active permeable materials. Interestingly, the sign of the A coefficient may be inverted using active permeable materials, although it appears that there are no solutions that allow it to be zero.

Rather than plotting R_W/R_D versus R_D, a plot of R_W versus R_D demonstrates the cloaking solutions for an active isotropic multilayer structure as in Fig. 6(a), or an active anisotropic multilayer structure as in Fig. 6(b). A single layer of active isotropic material is only able to reduce the effective radius of the wake by about 72%, while four layers are able to reduce the effective radius by 90%. The anisotropic cloaked solutions are likewise depicted in Fig. 6(b). Even though the single layer anisotropic structure has two degrees of freedom, the addition of a second layer of material increases the cloaking efficiency from 81% to 91%, which is approximately what is achievable by a four layer isotropic structure. The cloaking solutions can also be seen in Fig. 5(b), since the point where $R_A = R_D = 0$ also implies that $R_W = 0$, based on Eq. (72).

The velocity operator is able to convert these numerical results into streamlines that are much more illustrative of the mechanism of cloaking at work. In Figs. 7(a) and 7(b), we illustrate a five-layer cloak that was optimized using this Monte Carlo approach with an aspect ratio of two and a minimum normalized flow resistivity of $\rho' \equiv a^2\tilde{\rho} > -25$. The action of the layers serves to tighten the flow through the layers and correct the flow just outside the cloak so that it remains uniform everywhere except inside the cloak. In this particular case, the normalized flow resistivity of each of the five layers is given by $\rho' = (1.2821, -22.3214, -4.0552, 8.7032, 0.0010)$.

VII. ANALYSIS AND CONCLUSIONS

Wake and drag are closely related, but certainly distinct phenomena, and the purpose of this study is to show the extent to which they can be manipulated independently from each other in the linear (Stokes) limit. While the Stokes limit is the least complicated (and therefore less interesting) flow regime, it allows for the least computationally intensive

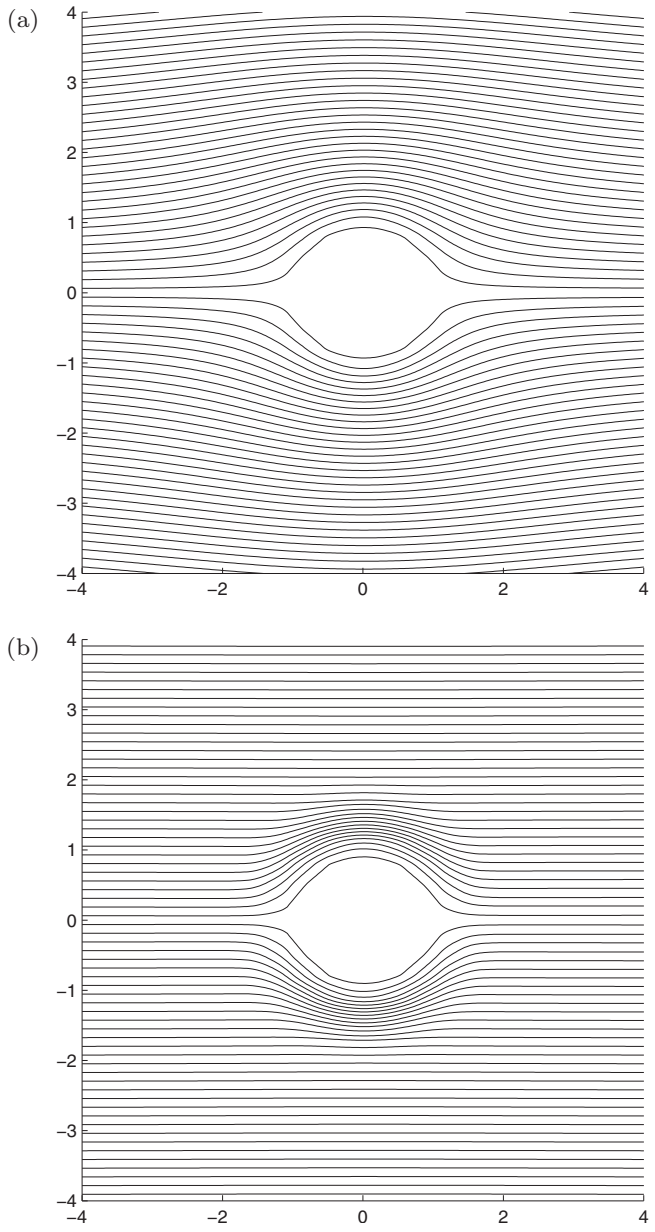

FIG. 7. Streamlines of an uncloaked (a) and an actively cloaked (b) sphere for a cloak with an aspect ratio of 2 and minimum $\rho' = -25$.

solution algorithms. Such algorithms can be adapted from electrodynamics, where linear problems have been in the focus for over a century, and readily exchanged with other disciplines where linear dynamics is important, such as acoustics and elastodynamics.

We emphasize that the conclusions derived from this study are limited to the case of uniform (plug) flow past and through a spherically symmetric object, and limited to small Reynolds numbers; these results cannot be applied outside of this domain without additional considerations. In this domain of applicability, the flow in the exterior region ($r > b$) is completely described by two real numbers: the coefficients $A_1 = A$ and $A_2 = B$, as defined in Sec. VI. This remains true regardless of the radial complexity of the system, as long as the system remains spherically symmetric. The latter requirement imposes a constraint on the orientation of the eigenvectors of the permeability tensor, which must be locally aligned with the spherical coordinate basis. The second of these coefficients (B) is entirely responsible for the drag force, which is linearly proportional to it. The extent to which this drag force coefficient can be controlled by a radial distribution of a passive permeable medium in a shell of given dimensions ($a < r < b$) is elucidated by Figs. 2(a), 2(c), 3(a), 3(b), 4(a), and 4(b). In short, this coefficient cannot be smaller than its value for an impermeable sphere of radius a; nor can it be larger than its value for a sphere of radius b. This remains valid even in the case of spherically anisotropic passive porous medium, as seen from Figs. 3(a), 3(b), 4(a), and 4(b). Both of these conclusions are in accord with our common sense. The first one is strictly mandated by the minimum dissipation theorem [30], which states that, with the given boundary conditions, the free-space Stokes flow dissipates less than any other flow, including the Brinkman-Stokes flow with any permeability distribution, or any other incompressible flow modified by external forces. This theorem follows directly from the form of the viscous dissipation functional [31], whose no-slip boundary-condition constrained minimum is achieved on a free Stokes flow.

We base our conclusions on numerical Monte Carlo (MC) samplings of the infinite space of all possible continuous radial permeability functions. These samplings are performed by first discretizing these one-dimensional functions on a finite grid, i.e., by replacing each continuous permeability function with a finite-dimensional parameter vector, and then selecting a large and therefore sufficiently representative set of parameter vectors. As can be seen from Fig. 2(a), there is rapid convergence towards a certain manifold in the space of two figures of merit (such as the norm of wake and the drag coefficient), as the number of discrete layers increases. This rapid and essentially monotonic convergence implies that the exterior flow parameters (A, B) are smooth functions of permeability, devoid of any oscillatory or resonant behavior.

As for the other coefficient ($A_1 = A$), which plays into the wake but has no effect on the drag, our intuition or energy arguments do not provide an intuitive answer; for example, it would be conceivable that this coefficient can be controlled to a greater extent than the B coefficient. The most extreme way of controlling this coefficient would be to cancel it entirely, which does not have to require making the B coefficient zero, or even reducing it by any amount. Our MC-based results reveal, however, that the A coefficient is substantially correlated with the B coefficient [Figs. 4(a) and 4(b)]. This correlation becomes much weaker as the number of layers (N) increases, or as the geometric aspect ratio of the shell (R_2/R_1) becomes large: the accessible combinations of (A, B) form a 1D curve at $N = 1$, but already at $N \geqslant 2$ they form a manifold of an ever-increasing area. This means that the A coefficient can be increased or decreased somewhat independently from the drag coefficient, to the maximum extent that depends on the shell aspect ratio. This translates into the ability to manipulate the norm of wake, which is defined in Sec. VI.

As seen in Figs. 3(a) and 3(b), at the aspect ratio of 5, we observe maximum variation of the norm of wake at a fixed drag coefficient, reaching about 3%. This maximum variation increases with the growing aspect ratio [Fig. 2(c)].

In Figs. 2(a), 2(c), 3(a), and 3(b), the norm of wake and the drag coefficient are represented by the equivalent wake radius (R_W) and equivalent drag radius (R_D), respectively, which correspond to the radii of an impervious simple sphere having the same norm of wake or the same drag force. Consequently, a passive porous sphere can be designed to have a smaller norm of wake than an impervious solid sphere having the same drag coefficient. Note that in the (R_W, R_D) coordinates, the impervious sphere is represented by a straight line $R_W = R_B$, or a horizontal line with $R_W/R_D = 1$ in the $(R_W/R_D, R_D)$ plots (Figs. 2 and 3). Since the two spheres with the same drag coefficient require an equal amount of power to be moved through a stationary fluid, this finding opens up an opportunity to reduce wake without any energy penalty.

Nevertheless, the A coefficient and the related kind of wake can only be changed in a certain range by a passive permeable medium, as our results reveal. In particular, its minimum and maximum values are still limited to the values of A coefficient for the impermeable spheres of radii a and b, respectively, much like the accessible range for the B coefficient. This conclusions remains true when spherical anisotropy of permeability is included.

These ranges change dramatically when an active medium, described by negative or indefinite permeability, is allowed. The first dramatic, although entirely expected [17] change is that the B coefficient can now be less than its value for the core sphere (an impervious sphere of radius (R_1); moreover, it can be negative, as seen from Fig. 5 (a). In this figure, the magenta dots correspond to the already discussed passive case; as the minimum permissible value of flow resistivity goes negative, the accessible domain in the wake-drag diagram becomes progressively wider, taller, and larger in area. The apparent singularity in the R_W/R_D at $R_D = 0$ is due to the denominator crossing zero.

Another interesting effect is observed in the A coefficient [Fig. 5(b)]. It is now possible to make it precisely zero, or positive, even when the drag coefficient is not small. However, cancellation of the A coefficient is only observed in the regime where R_D is approximately equal to a; therefore, it still essentially requires an active medium, which can bring R_D of a permeable sphere down to a.

A counterintuitive observation can be made from Fig. 5(b): the A coefficient remains somewhat correlated with the B coefficient, and the correlation becomes tighter as one moves away from the zero crossing for A. This correlation cannot be removed even with arbitrarily large amounts of external volumetric force that can be applied by the active medium. A similar correlation is seen for the norm of wake [Figs. 6(a) and 6(b)], which is dependent upon but not entirely determined by the A coefficient. For the norm of wake, complete decorrelation from the drag coefficient (and thus independent control) is only possible in the regime where the drag is nearly perfectly compensated by the active medium; see the insets in Figs. 6(a) and 6(b). In the latter regime, our MC samplings readily reveal a number of solutions with simultaneously small (A, B), similar to those found in [17]; one such solution is depicted in Figs. 7(a) and 7(b), where it is compared against a bare impervious sphere of radius a. These trial solutions can be further perfected using optimization techniques along the lines of Ref. [17,32].

Although the degree of independent control over both the wake and drag is somewhat limited when using passive permeable materials, the results presented in this work show the absolute limit of what might be done with the range of flows around an object that can be readily and exactly solved analytically, i.e., the Stokes flow regime with spherical symmetry. However, once the constraint of spherical symmetry is dropped, it has been shown that there is significantly more control over the wake and drag, and increasing the Reynolds number also increases the range of possible wake and drag values [33].

Even in the Stokes flow limit, solving the problem of the multilayer permeable sphere furthermore shows that there is a much greater degree of control over the wake and drag of a sphere if active permeable materials can be used, and this information will encourage the development of hydrodynamic metamaterials that may be able to achieve this range of material properties.

ACKNOWLEDGMENTS

This work was supported by the Office of Naval Research (ONR) of the U.S. Navy through the Multidisciplinary University Research Initiative (MURI), award N00014-13-1-0631, and partially through the Naval Undersea Research Program (formerly a University Laboratory Initiative), award N00014-13-1-0743. The authors acknowledge useful discussions with Dean Culver (Duke University).

[1] H. Stone, A. Stroock, and A. Ajdari, Engineering flows in small devices, Annu. Rev. Fluid Mech. **36**, 381 (2004).

[2] H. Brinkman, On the permeability of media consisting of closely packed porous particles, Appl. Sci. Res. **1**, 81 (1949).

[3] J. Bear, *Dynamics of Fluids in Porous Media*, Dover Civil and Mechanical Engineering Series (Dover Publications, Mineola, NY, 2013).

[4] D. Nield and A. Bejan, *Convection in Porous Media* (Springer, Berlin, 2012.

[5] N. F. M. Martins, Identification results for inverse source problems in unsteady Stokes flows, Inverse Probl. **31**, 015004 (2015).

[6] J. Prakash and G. P. Raja Sekhar, Arbitrary oscillatory Stokes flow past a porous sphere using Brinkman model, Meccanica **47**, 1079 (2012).

[7] T. Arbogast and H. Lehr, Homogenization of a Darcy-Stokes system modeling vuggy porous media, Comput. Geosci. **10**, 291 (2006).

[8] G. H. Neale and W. K. Nader, Prediction of transport processes within porous media: Creeping flow relative to a fixed swarm of spherical particles, AIChE J. **20**, 530 (1974).

[9] J. Rubinstein and S. Torquato, Flow in random porous media: Mathematical formulation, variational principles, and rigorous bounds, J. Fluid Mech. **206**, 25 (1989).

[10] H. Burcharth and O. Andersen, On the one-dimensional steady and unsteady porous flow equations, Coastal Eng. **24**, 233 (1995).

[11] H. C. Brinkman, A Calculation of the viscous force exerted by a flowing fluid on a dense swarm of particles, Appl. Sci. Res. **1**, 27 (1949).

[12] K. Matsumoto and A. Suganuma, Settling velocity of a permeable model floc, Chem. Eng. Sci. **32**, 445 (1977).

[13] J. H. Masliyah, G. Neale, K. Malysa, and T. G. V. D. Ven, Creeping flow over a composite sphere: Solid core with porous shell, Chem. Eng. Sci. **42**, 245 (1987).

[14] D. D. Joseph and L. N. Tao, The effect of permeability on the slow motion of a porous sphere in a viscous liquid, Z. Angew. Math. Mech. **44**, 361 (1964).

[15] P. Levresse, I. Manas-Zloczower, and D. Feke, Hydrodynamic analysis of porous spheres with infiltrated peripheral shells in linear flow fields, Chem. Eng. Sci. **56**, 3211 (2001).

[16] B. Padmavathi and T. Amaranath, A solution for the problem of stokes flow past a porous sphere, Z. Angew Math. Phys. **44**, 178 (1993).

[17] Y. A. Urzhumov and D. R. Smith, Fluid flow control with transformation media, Phys. Rev. Lett. **107**, 074501 (2011).

[18] H. Kim and K. Najafi, An electrically-driven, large-deflection, high-force, micro piston hydraulic actuator array for large-scale microfluidic systems, in *Proceedings of the IEEE International Conference on Micro Electro Mechanical Systems (MEMS)* (IEEE, 2009), pp. 483–486.

[19] C. Lee, G. Hong, Q. Ha, and S. Mallinson, A piezoelectrically actuated micro synthetic jet for active flow control, Sens. Actuators A Phys. **108**, 168 (2003), selected papers from the Pacific Rim Workshop on Transducers and Micro/Nano Technologies.

[20] H. van Lintel, F. van De Pol, and S. Bouwstra, A piezoelectric micropump based on micromachining of silicon, Sens. Actuators **15**, 153 (1988).

[21] R. Zengerle, J. Ulrich, S. Kluge, M. Richter, and A. Richter, A bidirectional silicon micropump, Sens. Actuators A Phys. **50**, 81 (1995).

[22] C. F. Bohren and D. R. Huffman, *Absorption and Scattering of Light by Small Particles* (Wiley, New York, 1983).

[23] O. Pea-Rodrguez, P. P. G. Prez, and U. Pal, Mielab: A software tool to perform calculations on the scattering of electromagnetic waves by multilayered spheres, Int. J. Spectrosc. **2011**, 10 (2011).

[24] W. Yang, Improved recursive algorithm for light scattering by a multilayered sphere, Appl. Opt. **42**, 1710 (2003).

[25] J. Koplik, H. Levine, and A. Zee, Viscosity renormalization in the brinkman equation, Phys. Fluids **26**, 2864 (1983).

[26] M. C. Troparevsky, A. S. Sabau, A. R. Lupini, and Z. Zhang, Transfer-matrix formalism for the calculation of optical response in multilayer systems: From coherent to incoherent interference, Opt. Express **18**, 24715 (2010).

[27] S. V. Zhukovsky, Perfect transmission and highly asymmetric light localization in photonic multilayers, Phys. Rev. A **81**, 053808 (2010).

[28] A. V. Zvyagin and K. Goto, Mie scattering of evanescent waves by a dielectric sphere: Comparison of multipole expansion and group-theory methods, J. Opt. Soc. Am. A **15**, 3003 (1998).

[29] J. Happel and H. Brenner, *Low Reynolds Number Hydrodynamics*, International Series in the Physical and Chemical Engineering Sciences (Prentice Hall, Englewood Cliffs, NJ, 1965).

[30] S. Kim and S. Karrila,. *Butterworth-Heinemann Series in Chemical Engineering* (Dover Publications, Mineola, 2005).

[31] Y.-M. Koh, Vorticity and viscous dissipation in an incompressible flow, KSME J. **8**, 35 (1994).

[32] Y. A. Urzhumov and D. R. Smith, Flow stabilization with active hydrodynamic cloaks, Phys. Rev. E **86**, 056313 (2012).

[33] D. R. Culver, E. Dowell, A. Varghese, D. R. Smith, and Y. Urzhumov, A volumetric approach to wake reduction: design, optimization, and experimental verification (unpublished).